The Eurasia Proceedings of Science, Technology, Engineering & Mathematics (EPSTEM)
ISSN: 2602-3199

The Eurasia Proceedings of Science, Technology, Engineering and Mathematics (EPSTEM), 2025

Volume 37, Pages 820-833

ICEAT 2025: International Conference on Engineering and Advanced Technology

Influence of Steel Plate on Enhancing the Punching Strength of Voided Slabs

Athmar M. Alazawiey
Wasit University

Thaar S. Al-Gasham
Wasit University

Sajjad H. Ali
Wasit University

Abstract: Punching failure is a possibility for the voided slabs, particularly when they are exposed to unbalanced moments. Thus, the purpose of this investigation is to provide a strengthening method involving the use of steel plates to strengthen the voided slab when it is subjected to an unbalanced moment. The structural performance, especially punching shear of a voided slab reinforced with a steel plate at the interior voided slab-column connections, was examined in this study. Four specimens were constructed using slabs that were 1100 × 1100 × 130 mm and had styropor voids distributed throughout them. A square column that was 250 mm high and with a cross section of 150 × 150 mm was extruded from the upper face of a slab center. An eccentric load was applied via a column stub and an integral beam section, measuring 150 mm by 150 mm, extruded 150 mm from the column face to simulate an unbalanced moment. By inserting two plates in each direction, four steel sheets were implanted into three specimens to reinforce them; the remaining slab was a control without steel plates for strengthening. As well, one slab without voids was created to be a reference of strength degradation due to void insertion. The two other specimens were one voided without steel plates and the other was solid without voids, used as a reference specimen. Near the column stub, these sheets crossed each other orthogonally. Eight square voids, each measuring 250 mm × 250 mm × 70 mm, were present in the voided specimens. They experimented till they failed under an unbalanced moment. Comparing the voided slab with a steel plate to the control slab without strengthening, the test results showed notable improvements in strength, about 8%, ductility to 146%, and toughness, reaching 18%.

Keywords: Voided slab, Unbalanced moment, Slab-column connections, Steel sheet, Punching failure

Introduction

Flat plate slabs are the most common in modern reinforced concrete (RC) structures, supported directly by columns without beams. This configuration offers advantages such as reduced building height, faster and simpler formwork, and improved service integration flexibility (Saleh et al., 2019). To meet deflection and punching shear requirements, these slabs are usually thick, leading to increased self-weight and uneconomical designs, especially for large spans (Al-Gasham et al., 2019). In response, various lightweight slab systems have been developed.

One notable solution is the voided slab system introduced in 1990 by Jørgen Breuning, which incorporates voids (often made of polystyrene or plastic) between reinforcement layers to remove inactive concrete and reduce weight by 30–35% while maintaining similar flexural strength (Al-Gasham et al., 2019; Chung, Jung, et al., 2018; Valivonis et al., 2014). These slabs, known as "bubble deck" or "biaxial slabs," are also environmentally

- This is an Open Access article distributed under the terms of the Creative Commons Attribution-Noncommercial 4.0 Unported License, permitting all non-commercial use, distribution, and reproduction in any medium, provided the original work is properly cited.

- Selection and peer-review under responsibility of the Organizing Committee of the Conference

© 2025 Published by ISRES Publishing: www.isres.org

beneficial due to reduced material use and the incorporation of recycled materials (Andrew, 2018).Extensive research over the past decade indicates that voided slabs offer comparable flexural strength to solid slabs when voids are placed in tensile zones (Chung et al., 2014; Chunget al., 2018; Ibrahim et al., 2013).

However, stiffness typically decreases by 10–20% (Ibrahim et al., 2013), and flexural capacity can drop by 11–20% depending on the void configuration (Chungü et al., 2018; Khouzani et al., 2021; Mahdi & Mohammed, 2021). More critically, voided slabs suffer from significantly reduced shear and punching strength up to 40% less in some cases, depending on the void type and location (Chung, Bae, et al., 2018; Chung et al., 2011; Oukaili & Merie, 2021; Sagadevan & Rao, 2019, 2022; Valivonis, Šneideris, et al., 2017). For example, spherical voids positioned close to columns led to 18–29% reductions in punching strength (Oukaili & Merie, 2021). Shape also matters; some void forms caused over 43% strength loss (Valivoniset al., 2017).

Though reinforcement techniques using steel fibers or GFRP sheets have shown improvements in punching strength and ductility (Al-Azzawi & Mtashar, 2023). The brittle punching failure remains a major concern. Traditional solutions—like adding complex solid zones around columns are labor-intensive and reduce the economic benefits of voided slabs. Furthermore, current studies do not demonstrate a fundamental change in the failure mechanism. Therefore, new strategies are needed to significantly improve the punching shear performance of voided slabs without compromising their structural and economic efficiency.

In the current work, a new method to enhance the punching strength of voided slabs was employed, instead of leaving solid parts around columns. In this method, steel plate sheets are inserted next to columns. These sheets are lower in cost, facilitate rapid construction, and maintain the lightweight of the voided slabs related to leaving solid parts around the columns, in addition to revolution to a ductile one instead of the sudden shear failure that continuously occurs in voids in slabs, even when shear bolts are utilized or voids are moved away from the column faces (Chunget al., 2018). In this paper, specimens were tested under unbalanced moments until failure. The results were then compared with those of the control and reference slabs for strength, deformation, ductility, and toughness.

Testing Program

Specimens' Description

A section of a voided flat plate situated in the area of the negative moment around an internal column within the contra-flexure line was represented by the model that was constructed. The Auto Desk Robot program was used to determine this area. The flat plate structure was supported by 16 columns that were spaced uniformly in the x and y axes. There were 5 meters between each column's center. The structure was then subjected to a load that was uniformly distributed. Figure 1 displays the results of the study, which demonstrate the moment distribution in the x-direction. As can be seen, the saddle point is 1.1 meters from the column's face when the negative moment is transverse to the positive moment. The tested samples were half-scale, due to the lab limits, positioned along the lower face of the sample on a supporting border that measured 1000 mm × 1000 mm. The applied vertical loads caused a negative moment on the sample's top surface and tension stresses in the bottom surface.

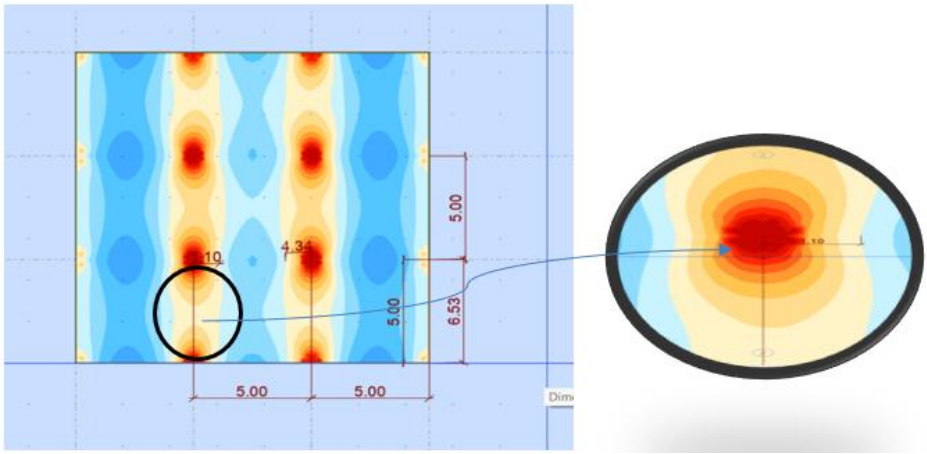

Figure 1. The specimen in the robot program

It is important to notice that the size of specimens is equivalent to those that Binici and Bayrak adopted (Binici & Bayrak, 2005).While the experimental procedure utilizes specimens with a linear scale. Programs using reinforced concrete elements are frequently implemented due to laboratory limitations; the size effect in scaled-down specimens causes the nominal shear stress to be larger than that in the equivalent full-scale one (Guandalini et al., 2009). Nevertheless, the impact of size on thin slabs (less than 400 mm thick) is minimal. It is dependent on a member's ability to transfer interior forces due to reinforcement yielding and cracking, in addition to the slab's thickness (Fernández Ruiz & Muttoni, 2018).

According to Table 1, a self-compacting concrete (SCC) mixture was used to cast the five samples, ensuring that the small spaces between the reinforcing bars were filled and preventing segregation. The produced self-compacting concrete mixture has been designed to reach a compressive strength (f_{cu}) of 40 MPa after 28 days of curing. The specimens created on a half scale were employed to fulfill the goal of this investigation. A central column inside the building is displayed, which is linked to a slab.

Table 1. Proportion of the mixed materials

Material	Quantity
Water/cement ratio	0.463
Water (kg/m^3)	185
Cement (kg/m^3)	400
Fine aggregate (kg/m^3)	1060
Coarse aggregate (kg/m^3)	586
Limestone Powder (kg/m^3)	70
Superplasticizer (kg/m^3)	12

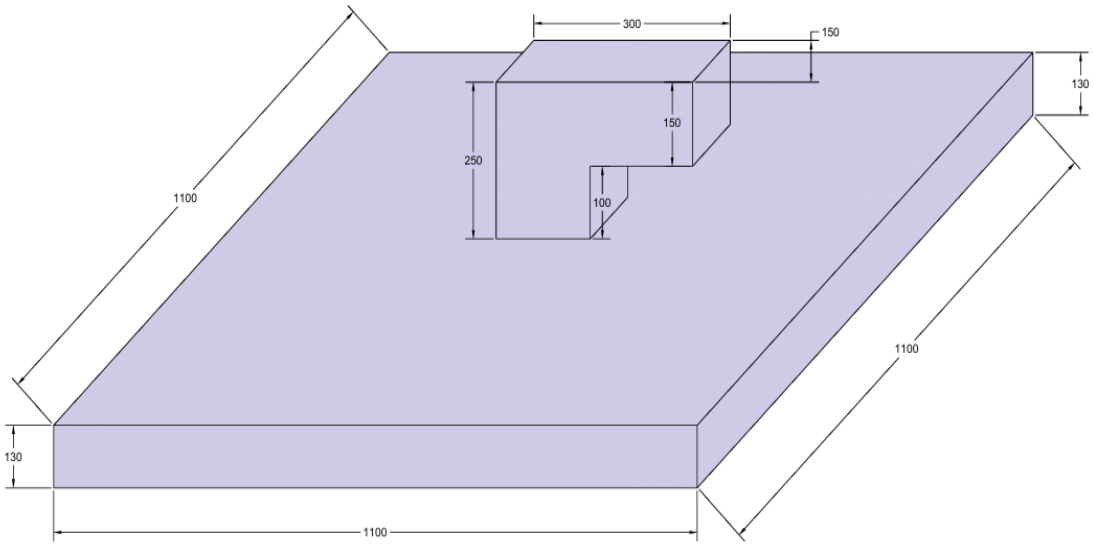

Figure 2. The dimension of the specimen

Two layers of 8 mm steel bars, spaced center to center at 100 mm in both directions, served as reinforcement for every specimen. An effective depth (*dav.*) of 108 mm was provided by the placement of the two layers. Five square ties composed of 8 mm steel bars served as the transverse reinforcement for the columns, while 10Ø12 mm was used for the longitudinal bar. The transverse bar of the beam was two square stirrups constructed of an 8 mm steel bar, while the longitudinal reinforcement was 3Ø12 at the top bar and 2Ø12 at the bottom, as displayed in Figure 3. The used steel bar was examined according to ASTM C370-05. Table 2 lists the resulting ultimate and yield strength stress.

Table 2. Steel bar properties

Nominal diameter (mm)	Measured diameter (mm)	Yield Stress f_y MPa	Ultimate Strength f_u MPa	Elongation
8	7.7	516	577.5	13.935
12	12	616.5	687.31	11.35

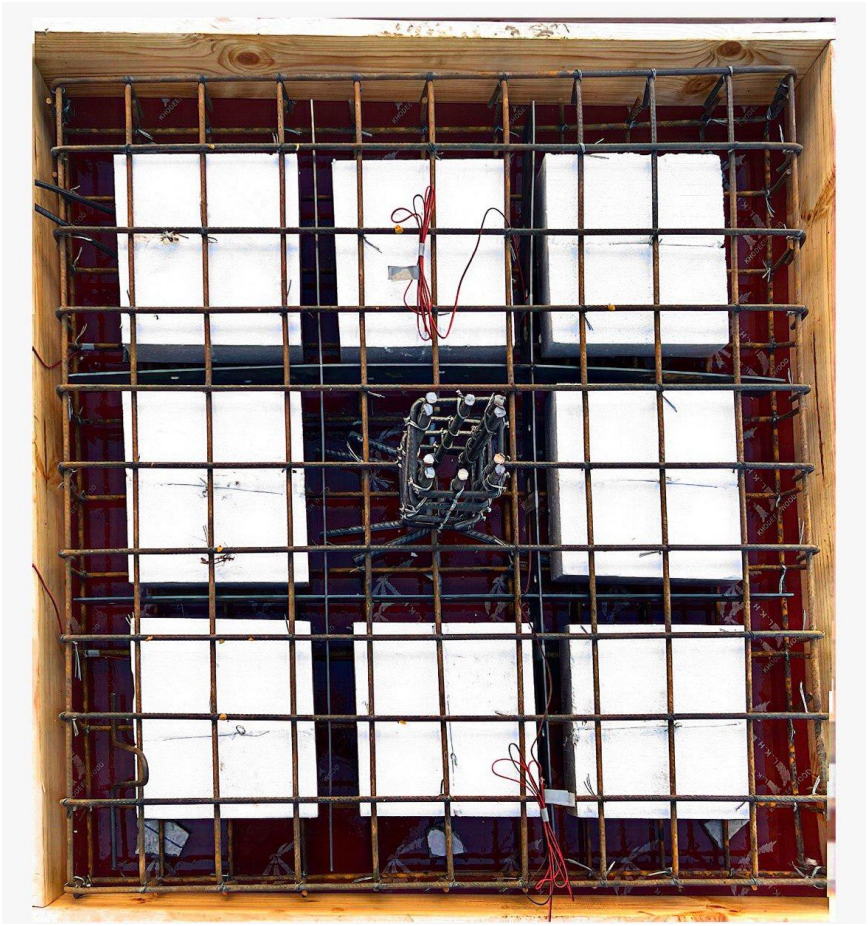

Figure 3. Reinforcement of the prepared sample

Eight styropor blocks measuring 250 x 250 mm in cross sections and 70 mm in height were utilized to create voids inside the slabs. Three lines of styropor blocks were placed equally separate from one another. There was a 50 mm clear distance between each pair of blocks. The prepared voided slab's planning is displayed in Figure 4.

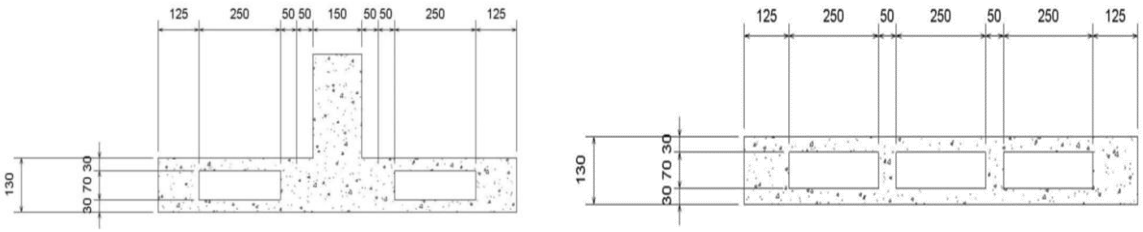

Figure 4. Arrangement of the voided slab

Specimens of the Study

Five reinforced self-compacting concrete slabs were cast to investigate the influence of thickness and steel plate arrangement on the resulting structural response, particularly the punching shear capacity of voided slabs. The designation of the prepared specimens is shown in Figure 5. One slab was made with a solid area, free of voids, which served as the control specimen; the remaining slabs were voided by distributing 8 square voids within them. One of the voided slabs was without a steel plate; three of them were reinforced by steel sheets with various thicknesses (1 mm, 2mm, and 3mm), as shown in Figure 6. The designation for the voided slabs included the letter (V) follow it the number that denoting to the thickness of the steel strip (i.e., V0= voided slab without steel strips and V1=voided slab with steel plate with thickness of a 1 mm, V2= voided slab with steel plate with thickness of a 2 mm, V3= voided slab with steel plate with thickness of 3 mm.

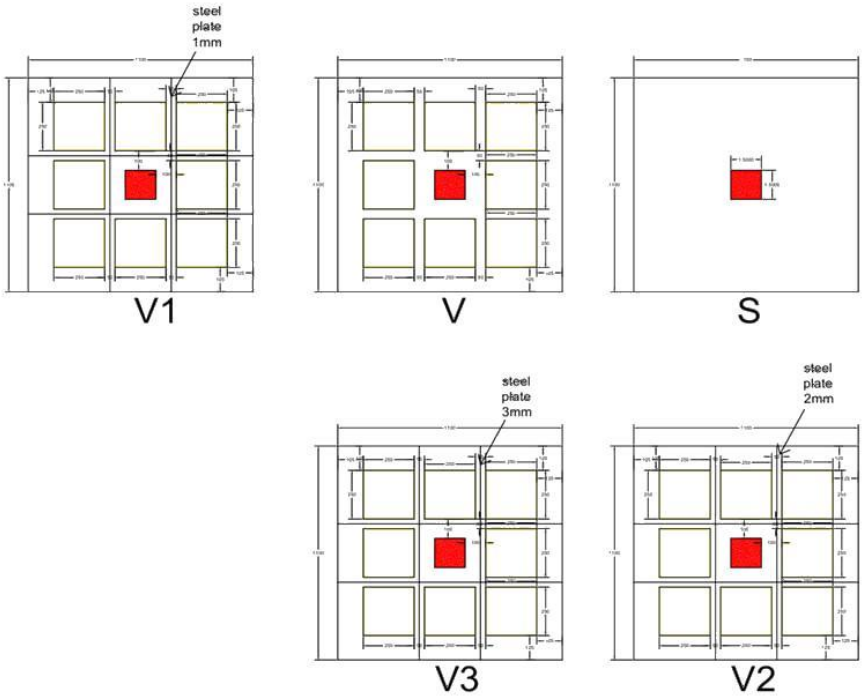

Figure 5. The designation of the prepared specimens and arrangement of steel thickness

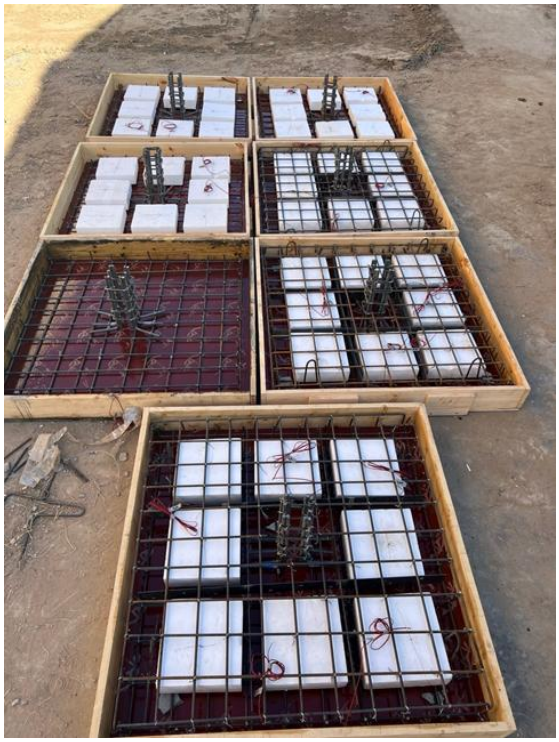

Figure 6. The experimental specimens

Each longitudinal and transverse direction has two stirrups. To confirm the demand development length, the complete length of the 1000 mm specimen was extended, with the two steel plate strips positioned in the middle of the two middle ribs in both directions. Additionally, these four strips have been connected around the column stub in an orthogonal way. Furthermore, these 68 mm high strips have been placed directly between the top and lower reinforcement layers. The concept of anchoring the sheets with holes was proposed by (Lameiras et al., 2018). They suggested that the diameter of the holes must exceed the maximum size of aggregate, and that bond strength improves with an increase in the number of holes. No guidance was provided on the spacing between holes. In this study, the diameter of the holes was chosen to be approximately 50% larger than the maximum size of aggregate (10 mm). This diameter appears appropriate (approximately 22% of the sheet's height) for

minimizing the cut area from the sheets. Two lines of 15 mm holes were punched into the sheets to facilitate the entry of aggregate into the slabs. The sheets were to be affixed to the slab at intervals of d (the distance between two subsequent holes) as the spacing between holes in a single line was almost equal to 2d. As shown in Figure 7, the holes were evenly distributed in a staggered pattern over the strips, with a 200 mm center-to-center spacing and a 25 mm distance between the two lines. The yield strength of the steel sheets was nearly identical, averaging 310.33 MPa.

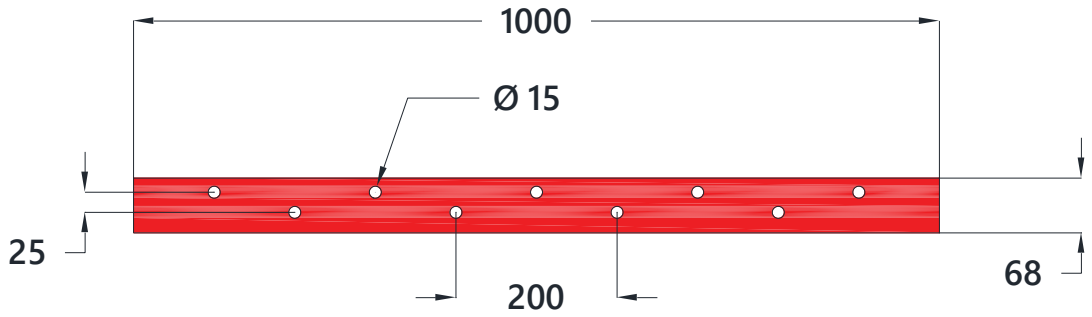

Figure 7. Details of the steel sheets

The strips must then be precisely assembled by overlapping the slots in order to strengthen the slab. To ensure a solid bond between the four parts, these overlapping connections had to be welded, as seen in Figure 8.

Figure 8. Details of the welding line in steel plates

Test Configuration and Instrumentation

At 28 days following casting, all the slabs experience an unbalanced moment load test, as shown in Figure 9. The beam-column area was used for the test. This force was applied using a hydraulic jack with a 2000 kN capacity until the specimen gradually collapsed. The displacement-controlled method was used to apply the eccentric load at a speed of 0.5 mm/min. To create a perimeter with a 1000 mm clear span, the slab specimens were positioned on roller lines along the four slabs' edges. The sample corners were free to raise throughout the test. This step is sufficient to capture the actual behavior of specimens located within the contra flexural lines, where the moments are zero.

Figure 9. Test setup

This configuration has been used in almost all of the punching shear studies since the 1950s (Muttoni, 2008). The force applied was measured using a load cell that was positioned between the column stub and the hydraulic jack piston. In order to measure the specimens' central deflection, a linear variable differential transducer, or LVDT, was located in the mid under the sample, exactly beneath the column's center. Strain gauges attached to the center lower bars in both longitudinal and transverse orientations were used to measure the tension bar strain next to the column edges. Also, strain gauges were positioned on the steel plates at the center. Finally, every tool used for recording test results was linked to a data logger, the Data logger G85, which took measurements. The readings were delivered directly to a computer at every second of the test.

Test Results and Description

Cracking Pattern and Failure Mode

The flexural cracks in the solid specimens (S) were initially noticed on the bottom face (tension surface). At first, tiny flexural cracks appeared in the central area of the specimens, and their direction was perpendicular to the steel bars. More tangential and radial cracks appeared when the applied load increased; these cracks extended into the edge of the specimens. As the load was amplified, diagonal cracks appeared and developed from the angle of the column toward the spicemen's edge. Upon collapse, the specimen displayed the brittle and abrupt punching shear failure mode, with the diagonal cracks integrated (refer to Fig. 10a). The punched shear failure surface developed on the tension face at an average distance of 1.85 d (199.8mm) from the exterior edges of the columns. The specimen that was voided and did not contain steel sheets (V0) also failed in the punching shear. Related to the solid specimen (S), this specimen had significantly fewer cracks. As shown in Figure 10b, this is because there is an inverse relationship between the number of voids and cracks. Additionally, the shear failure border of the V0 specimen was the same distance from column face as the S specimen, with spacing of 199.8 mm (1.85d) from the column edge.

The other specimens (V1, V2, and V3), which had embedded steel sheets with thicknesses of 1 mm,2mm, and 3mm, showed similarly distributed cracks. This is entirely at odds with what was observed in the S and V0 specimens, where further diagonal cracks originated in the specimens' centers and extended towards their edges and corners. Nevertheless, the width of the cracks was significantly smaller than that of the cracks detected in the solid specimen (S). Due to the increasing applied stress, more diagonal cracks appeared, with the oldest ones reaching farther into the supporting lines, and the column stub penetrating the specimens to a depth of almost half of the slab before they failed. Because of the steel sheets, the column stub could be supported, and its load was distributed to other areas of the slab that could withstand even greater loads. Several irregularly shaped tangential cracks extended around the column just before it collapsed. Then, as display in Figures 10 b, c, d, and e, the specimens failed gradually and ductily due to a combined punching-flexural failure mechanism. From what we could tell by looking at the spot where the concrete spalled off, the reinforced slabs did not exhibit any

significant slippage between the sheet ductility and the concrete. Therefore, incorporating steel sheets proved a highly efficient method for enhancing the failure mode by moving it to ductile failure instead of the brittle failure that occurs in voided slabs, regardless of how far away the voids are from the column sides or the usage of shear bolts (Chung, Bae, et al., 2018; Han & Lee, 2014; Valivonis et al., 2017)

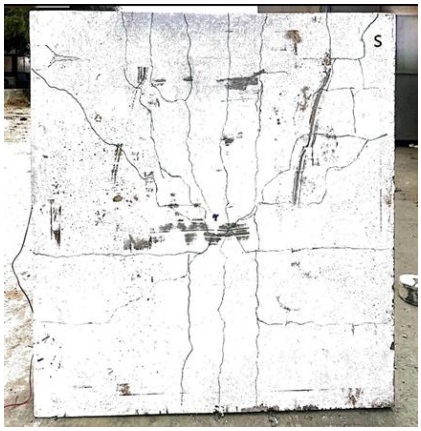

(a) S

(b) V0

(c) V1

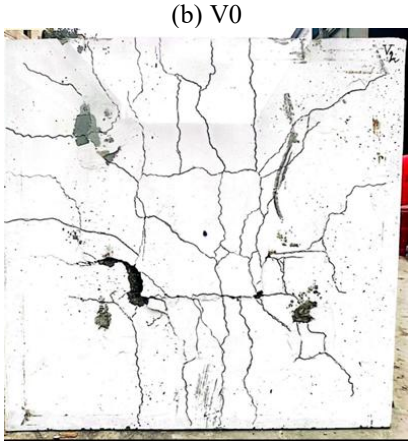

(d) V2

(e)V3

Figure 10. Crack pattern at failure loads

Load-Deflection Performance

General Behavior

The performance of the five experimental slab-column connections to load-central deflection is shown in Figure 11. It has come to light that reinforcement voided slabs with embedded steel plates caused these slabs' responses to differ significantly from those of other slabs (S and V0) that do not contain sheets. The S and V0.0

specimens' responses were two phases, pre-cracking and post-cracking. It all began with the pre-cracking stage, which was initiated at the start of the experiment till the first flexural cracking started to form. Then, as expected, the second phase, the post-cracking stage—began and sustained till the final boundary condition (ultimate limit state), where the stiffness decreased due to cracking. As a final point, the load capacity was severely reduced due to the slab being punched by the column stub in a brittle way.

The load-deflection responses for the samples reinforced with steel sheets (V1, V2, and V3) differed significantly from the recent explanations, primarily due to the presence of the steel sheets. There were four distinct phases to these responses. Similar to the S and V0 samples, the first two phases were also seen. In the third stage, the load-carrying capacity of the voided slab decreases as the loads go from ultimate to forces, which are around 50% of the peak loads. The reason for this behavior is that the concrete under the column stub is entirely cracking and failing to withstand further loads. Additionally, the steel plates in the central region, located under and around the column stub, also yielded.

On the other hand, these sheets reduced the column's sudden penetration of the slabs and transferred the applied force to the farther-off portions that could support greater loads. Next is stage four, where the centre deflection increased significantly without a corresponding change in the applied force. This stage is identified as the plastic plateau. The plastic plateau zone describes the point at which the ductility of voided slabs is significantly enhanced due to the employment of steel sheets for punching shear failure reinforcement. As a result of a combined flexural-punching failure, these three specimens exhibited a more ductile and progressive failure mechanism at the end of the tests. It is important to observe that the failure load and the ultimate load were not equivalent in the steel sheet-filled voided slabs. The loads were failure-accruing around 50% of the equivalent ultimate load. In difference, for both S and V0 slab samples, these two loads were identical.

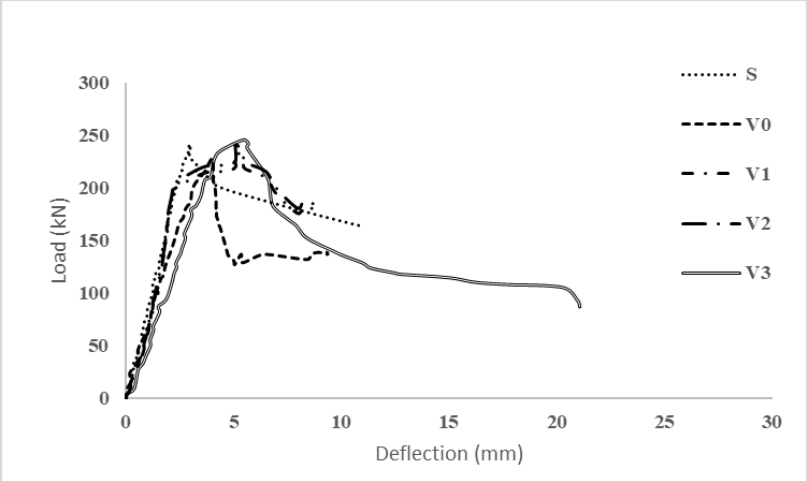

Figure 11. Force-deflection curve of specimens.

Ultimate Loads

The ultimate loads of each specimen are summarized in Table 3, and Fig. 11 plots these values against the thickness of the steel sheet. A closer look at the figure reveals that inserting eight voids across the total area of the V0 sample results in a reduction in the ultimate load of almost 5%, comparable to the S sample. This result was predicted because the critical area surrounding the column, primarily responsible for withstanding the punching loads generated in this region, still existed even in the case of inserting voids in the specimen.In addition, the steel sheet reinforcement for the voided slabs increased their strength and exceeded the missing strength due to the voids inserted across the slab-column joint. The spicemen V1 shows the same ultimate strength as the solid one. The remaining specimens were strengthened by 2 mm and 3mm; sheets showed a slightly higher ultimate load by approximately 1% and 3%, respectively. This slight increase is due to sheets being introduced far away from the column stub, where the concentrated stress is relatively low, which does not affect the strength of slabs. There are several possible explanations for this increase in strength. The first is that the steel sheets contained the concrete, which prevented the diagonal and flexural fractures from spreading further. The second factor stems from the significant vertical forces these plates provided, which helped withstand the punching power. The last consideration was the load-bearing capacity of these sheets, from the severely damaged region under and close to the column stub to the distant ones. The steel sheets also had four

corners to support them, which allowed them to act as direct struts to a certain degree and transmit some of the applied load to the borders that provide support. In practice, the transfer of loads from the slab to the supporting column is the inverse of what happens in the test setting. Since the sheets are lying on the supporting columns, they can also give direct support in the real situation. Finally, the voided slabs' flexural strength was enhanced because the steel plates served as flexural reinforcement.

Table 3. Test outcomes of samples

Sample	Ultimate load, Pu, (kN)	Yield deflection, Δy , (mm)[a]	Ultimate deflection, Δu, (mm)[b]	Ductility Index	Toughness kN mm
S	240	2.5	4.1	1.64	123
V0	228	3.5	4.1	1.17	138
V1	235	2.6	6.7	2.57	158
V2	242	2.5	7.2	2.88	163
V3	246	4	6.5	1.65	146

[a] founded by an equivalent elastic-plastic energy absorption method.
[b] founded by the crack method.

Deflection

As seen in Figure 10, the difference in the deflection between the seven specimens was particularly noticeable after the initial cracking. All specimens had nearly identical deflections before the cracking at the linear stage. Following that, the slab V0.0 displayed a soft response to load deflection, while the voided slabs with steel plates were the stiffest. Discussing the deflection at the same load is more suitable for a more precise description. Here, the service load accounts for 65% of the solid sample's peak load (156 kN), which was taken into account when calculating the deflection. At the service load, the V0 slab sample deflection was 25 % greater than the S specimen's. Nevertheless, this specimen collapsed at a load of less than 240 kN. This point highlights that the voided slab stiffness was severely decreased due to the rapid extension and growth of cracks through these voids.

The V1 specimen, strengthened by one mm-thick sheets, had a deflection equal to 3% , at the service load, smaller than that of the S specimen. For the remaining specimens, V2 and V3, at the service stage, the deflections were 5% and 14%, respectively, below those of the S specimen. These results show that the stiffness deterioration of the voids in slabs was completely mitigated by steel sheets, which limited the propagation and growth of both shear and flexural cracks. Additionally, these sheet plates worked instantaneously with flexural and shear reinforcement. They later improved the active moment of inertia of slab specimens, resulting in a considerable improvement in stiffness and a reduction in deflection rates.

Ductility

The Ductility index presented the relation of ultimate deflection (Δu) to yield deflection (Δy). The ductility index, yield, and ultimate deflections that were determined are listed in Table 3. The ductility of bubbling members was determined by (Hashemi et al., 2018) using the equivalent elasto-plastic energy absorption approach. This technique idealizes the experimental load-displacement curve into an elastic, perfect plastic curve that absorbs the same amount of energy as the real System (Figure 12a). This definition is used here because it appears reasonable. Additionally, (Park, 1989) detailed four processes for the final deflection. The method was selected after the work of (Hashemi et al., 2018). It depends on the first element crack (Figure 12b).

A significant loss in ductility was observed due to voids in the slab-column connection, about 29% compared to the solid sample (S). Voided slabs have a limited capacity to absorb seismic energy. Therefore, more care must be taken while building such slabs in seismic zones. Nevertheless, it was discovered that reinforcing the voided slabs with steel plates may offset this decline in the ductility index. So, the suggested use of steel sheets for voided slabs is an admirable solution for voided slabs subjected to seismic loads. However, the ductility improvement decreased as the sheet plate thickness increased, because the sheets served as extra flexural reinforcement; this effect became more pronounced as the sheet size increased. The steel thickness may cause the tension bars to take longer to yield. The ductility enhancement for the V1, V2, and V3 specimens were120 %, 146m%, and 41%, compared to the V0 slab, respectively.

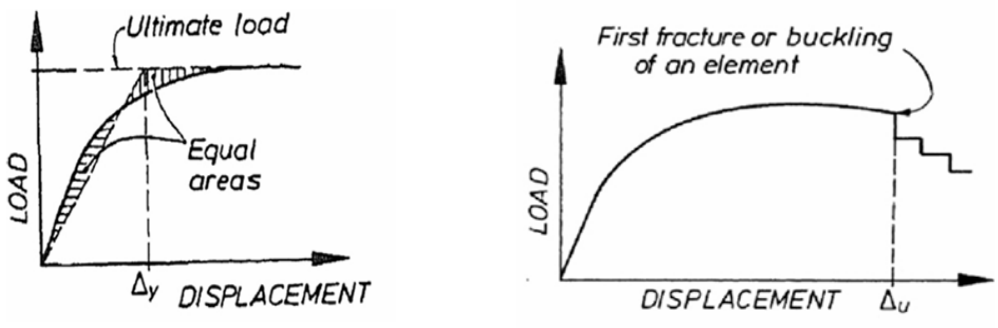

(a) (b)

Figure 12. Park's explanation for deflections (a) Description of yield displacement dependent on equal elasto-plastic energy absorption, (b) description of the ultimate deflection depended on the first crack of an element [27]

Toughness

The area enclosed by the load-deflection curve is representative of the toughness or energy absorption. Table 3 lists the energy absorbance values for each sample. The specimen's voids (V0) resulted in a high capacity of energy absorption, reaching 12%, in contrast to the solid slab (S); this is an increase in V0 because the energy absorption depended on the area under the curve of load-displacement, and V0 give a high deflection which provide a higher area and the toughness were measured up to failure not up to ultimate. Also, due to the solid area around the column stub, which omits the adverse effect of the voids present. As sheet thickness increased, the rate of energy absorption development slowed. Compared to the S specimen, the V1, V2, and V3 had energy absorptions of 29%, 33%, and 19%, respectively.

Stiffness

In a previous study, different methods were used to determine stiffness. The drop in stiffness usually occurs when the applied load becomes 75% of the failure load. Consequently, the slope of the line connecting the load-deflection curve's origin to 75% of the ultimate load was used to characterize the samples' stiffness as shown in Figure 13.

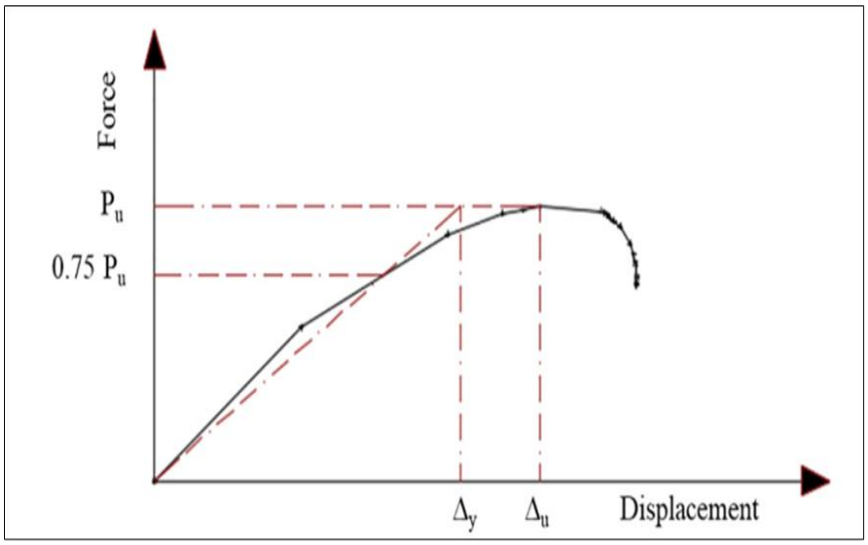

Figure 12. Methods that used to estimate the ductility and stiffness of the specimens

Table 4 includes the stiffness of specimens. As shown, stiffness is degraded in the voided sample because the voids rapidly develop and expand cracks throughout the specimen. As a result, the specimens' inertia moment decreased, causing degrading their stiffness. Voids influenced the connection stiffness remarkably, about 20%, which was found for specimen V0 compared with solid specimens S. The strengthened specimens with steel

sheet show enhancement in stiffness compared with the voided slab without a steel plate, about 28%,31%, and 39 %, for V1, V2, and V3, respectively.

Table 4. Stiffness results

Specimen	Stiffness (kN/m)
	75
V0	60
V1	76.9
V2	78.3
V3	83.3

Conclusion

The usage of a steel plate inserted inside the slabs. This study presented a novel and easy way to improve the reinforced concrete voided slab column connectors' punching strength and behavior when they are subjected to unbalanced moments. Five specimens were built as part of an experimental program that involved applying eccentric load through the beam-column stub until they failed. Four slabs were voided by distribution 8 Square voids within them, while one slab was constructed with a solid section without voids. Steel sheets that were 1 mm,2 mm, and 3 mm thick were used to reinforce three of them. Based on the results observed from the experimental study, the following are crucial conclusions.

1. A rapid and brittle punching shear mode caused the solid slab and the voided slab without steel sheets to collapse, but the slabs with steel sheets displayed a more ductile failure mode (combined flexural-punching mode).
2. The strength of the V0 voided slab was 5% less than that of the solid specimen S. The reinforced specimens V2 and V3 achieved ultimate loads that were 1% and 3% greater than those of the S slab; however, this loss was recovered and passed by employing the steel sheets. The spicemen V1 shows the same ultimate strength as the solid one. This slight increase is due to sheets being introduced far from the column stub, in a region with moderately low stress concentration, and does not affect the slabs' strength.
3. Because of the voids present, allowed cracking to start and spread rapidly, the V0 slab showed the least load-deflection response out of the five. However, under the tested conditions, the reinforced slabs exhibited the stiffest response because steel sheets could prevent cracks from spreading and expanding.
4. The use of steel plates increased the ductility index by 41% to 146% relative to the unreinforced voided slab, successfully restoring and exceeding the ductility of the solid slab.
5. The use of steel plates enhances stiffness by about 28%, 31%, and 39 %, for V1, V2, and V3, respectively compared with the voided slab without a steel plate.

Scientific Ethics Declaration

* The authors declare that the scientific ethical and legal responsibility of this article published in EPSTEM journal belongs to the authors.

Conflict of Interest

* The authors declare that they have no conflicts of interest

Funding

* This research received no specific grant from any funding agency in the public, commercial, or not-for-profit sectors.

Acknowledgements or Notes

* This article was presented as an oral presentation at the International Conference on Engineering and Advanced Technology (ICEAT) held in Selangor, Malaysia on July 23-24, 2025.

References

Al-Azzawi, A. A., & Mtashar, S. H. (2023). Behavior of two-way reinforced concrete voided slabs enhanced by steel fibers and GFRP sheets under repeated loading. *Results in Engineering*, *17*, 100872.

Al-Gasham, T. S., Hilo, A. N., & Alawsi, M. A. (2019). Structural behavior of reinforced concrete one-way slabs voided by polystyrene balls. *Case Studies in Construction Materials*, *11*, e00292.

Al-Gasham, T. S., Mhalhal, J. M., & Jabir, H. A. (2019). Improving punching behavior of interior voided slab-column connections using steel sheets. *Engineering Structures*, *199*, 109614.

Andrew, R. M. (2018). Global CO2 emissions from cement production. *Earth System Science Data*, *10*(1), 195–217.

Binici, B., & Bayrak, O. (2005). Upgrading of slab–column connections using fiber reinforced polymers. *Engineering Structures*, *27*(1), 97–107.

Chung, J.-H., Bae, B.-I., Choi, H.-K., Jung, H.-S., & Choi, C.-S. (2018). Evaluation of punching shear strength of voided slabs considering the effect of the ratio b0/d. *Engineering Structures*, *164*, 70–81.

Chung, J.-H., Choi, H.-K., Lee, S.-C., & Choi, C.-S. (2011). Shear capacity of biaxial hollow slab with donut type hollow sphere. *Procedia Engineering*, *14*, 2219–2222.

Chung, J.-H., Choi, H.-K., Lee, S.-C., & Choi, C.-S. (2014). Flexural strength and stiffness of biaxial hollow slab with donut type hollow sphere. *Journal of the Architectural Institute of Korea Structure & Construction*, *30*(5), 3–11.

Chung, J.-H., Jung, H.-S., Bae, B.-I., Choi, C.-S., & Choi, H.-K. (2018). Two-way flexural behavior of donut-type voided slabs. *International Journal of Concrete Structures and Materials*, *12*(1), 26.

Fernández Ruiz, M., & Muttoni, A. (2018). Size effect in shear and punching shear failures of concrete members without transverse reinforcement: Differences between statically determinate members and redundant structures. *Structural Concrete*, *19*(1), 65–75.

Guandalini, S., Burdet, O. L., & Muttoni, A. (2009). Punching tests of slabs with low reinforcement ratios. *ACI Structural Journal*, *106*(1), 87.

Han, S. W., & Lee, C. S. (2014). Evaluation of punching shear strength of voided transfer slabs. *Magazine of Concrete Research*, *66*(21), 1116–1128.

Hashemi, S. S., Sadeghi, K., Vaghefi, M., & Siadat, S. A. (2018). Evaluation of ductility of RC structures constructed with bubble deck system. *International Journal of Civil Engineering*, *16*(5), 513–526.

Ibrahim, A. M., Ali, N. K., & Salman, W. D. (2013). Flexural capacities of reinforced concrete two-way bubbledeck slabs of plastic spherical voids. *Diyala Journal of Engineering Sciences*, 9–20.

Khouzani, M. A., Zeynalian, M., Hashemi, M., Mostofinejad, D., Farahbod, F., & Shahadifar, M. (2021). A numerical study on flexural behavior of biaxial voided slabs containing steel cages. *Journal of Building Engineering*, *44*, 103382.

Lameiras, R., Valente, I. B., Barros, J. A., Azenha, M., & Goncalves, C. (2018). Pull-out behaviour of Glass-Fibre Reinforced Polymer perforated plate connectors embedded in concrete. Part I: Experimental program. *Construction and Building Materials*, *162*, 155–169.

Mahdi, A. S., & Mohammed, S. D. (2021). Structural behavior of BubbleDeck slab under uniformly distributed load. *Civil Engineering Journal*, *7*(2), 304–319.

Muttoni, A. (2008). Punching shear strength of reinforced concrete slabs without transverse reinforcement. *ACI Structural Journal*, *105*(4), 440.

Oukaili, N. K., & Merie, H. D. (2021). CFRP strengthening efficiency on enhancement punching shear resistance of RC bubbled slabs with openings. *Case Studies in Construction Materials*, *15*, e00641.

Park, R. (1989). Evaluation of ductility of structures and structural assemblages from laboratory testing. *Bulletin of the New Zealand Society for Earthquake Engineering*, *22*(3), 155–166.

Sagadevan, R., & Rao, B. (2019). Experimental and analytical investigation of punching shear capacity of biaxial voided slabs. *Structures*, *20*, 340–352.

Sagadevan, R., & Rao, B. (2022). Punching shear capacity of RC biaxial voided slab–prediction by critical shear crack theory. *ASPS Conference Proceedings*, *1*(2), 411–415.

Saleh, H., Kalfat, R., Abdouka, K., & Al-Mahaidi, R. (2019). Punching shear strengthening of RC slabs using L-CFRP laminates. *Engineering Structures*, *194*, 274–289.

Valivonis, J., Jonaitis, B., Zavalis, R., Skuturna, T., & Šneideris, A. (2014). Flexural capacity and stiffness of monolithic biaxial hollow slabs. *Journal of Civil Engineering and Management*, *20*(5), 693–701.

Valivonis, J., Skuturna, T., Daugevičius, M., & Šneideris, A. (2017). Punching shear strength of reinforced concrete slabs with plastic void formers. *Construction and Building Materials*, *145*, 518–527.

Valivonis, J., Šneideris, A., Šalna, R., Popov, V., Daugevicius, M., & Jonaitis, B. (2017). Punching strength of biaxial voided slabs. *ACI Structural Journal*, *114*(6), 1373–1383.

Author(s) Information

Athmar M. Alazawiey
Wasit University, College of Engineering, Wasit, Iraq
Contact: Std2023203.A.M@uowasit.edu.iq

Thaar S. Al-Gasham
Wasit University, College of Engineering, Wasit, Iraq

Sajjad H. Ali
Wasit University, College of Engineering, Wasit, Iraq,

To cite this article:

Alazawiey, A. M., Al-Gasham, T. S., & Ali, S. H. (2025). Influence of steel plate on enhancing the punching strength of voided slabs. *The Eurasia Proceedings of Science, Technology, Engineering and Mathematics (EPSTEM), 37,* 820-833.